Shahid Bahonar University of Kerman
Agricultural Biotechnology Journal
Iranian Biotechnology Society
Print ISSN: 2228-6705 Online ISSN: 2228-6500

Integrated protein and gene expression analysis of S100A1 and S100A8/A9 demonstrates coordinated dysregulation of calcium homeostasis, innate immune activation, and angiogenic signaling in acute Myocardial infarction

Elham F. Hamzah
* Corresponding author. Department of Clinical Biochemistry, Hammurabi College of Medicine, Babylon, University, Hillah, Iraq. E-mail: if0261758@gmail.com
Abdulsamie Hassan Alta'ee
College of Medicine, Babylon University, Hillah, Iraq. E-mail: abdulsamie68@gmail.com
Ameer Aljubawii
College of Medicine, Babylon University, Hillah, Iraq. E-mail: aljubawiiameer1981@gmail.com

Abstract

Objective

Acute myocardial infarction (AMI) is characterized by complex molecular interactions involving disruption of cardiomyocyte calcium homeostasis, activation of innate immune pathways and impaired angiogenic signaling. However, the integrated relationship between the cardiomyocyte-specific S100A1 protein and the inflammatory S100 A8/A9 complex remains incompletely understood. Thus, this study aimed to evaluate the protein and gene expression profiles of S100A1 and S100A8/A9 and their association with inflammatory (TNF-α) and angiogenic (VEGF-A) biomarkers in AMI.

Materials and methods

This case-control study included 176 participants (88 AMI patients and 88 age and sex matched controls). Participants were recruited from AL-Hilla Teaching Hospital and Marjan Medical City. Circulating levels of S100A1, S100A8/A9, TNF-α and VEGF-A were measured using ELISA, while serum calcium was quantified with spectrophotometry. Gene expression levels of *S100A1, S100A8* and *S100A9* were determined by qRT-PCR using 2^−ΔΔCt method. Apply receiver operating characteristic (ROC) curve analysis to assess diagnostic performance.

Results

Significant multi-axis dysregulation was observed in AMI patients. *S100A1* mRNA expression was markedly reduced ($p<0.0001$), accompanied by decreased circulating S100A1 protein (AUC = 0.69Y, specificity = 100%). In contrast, inflammatory markers were elevated with S100A8/A9 demonstrating acceptable diagnostic performance (AUC=0.76), while TNF-α showed no discriminative value (AUC=0.50). Serum calcium exhibited strong diagnostic accuracy

(AUC=0.82), indicating early disruption of calcium homeostasis. Angiogenic impairment was reflected by reduced VEGF-A levels but with limited diagnostic utility (AUC = 0.54). Gene expression analysis further confirmed significant upregulation of *S100A8* (p=0.030) and *S100A9* (p=0.044). No significant correlation was observed between S100A1 and inflammatory markers (p>0.05), whereas *S100A8* and *S100A9* expression showed a strong positive association, indicating coordinated inflammatory activation.

Conclusion

These findings show that calcium control linked to S100A1, immune responses from S100A8/A9 and issues with blood vessel formation related to VEGF-A are all connected. The superior diagnostic capability of S100A1 suggests that markers reflecting calcium management in cardiac cells may enhance the identification of acute myocardial infarction (AMI) and provide greater insight than conventional inflammatory indicators.

Keywords: acute myocardial infarction, calcium, gene expression, TNF-α, VEGF-A

Paper Type: Research Paper.

Citation: Hamzah, E. F., Alta'ee, A. H., & Aljubawii, A. (2026). Integrated protein and gene expression analysis of S100A1 and S100A8/A9 demonstrates coordinated dysregulation of calcium homeostasis, innate immune activation, and angiogenic signaling in acute Myocardial infarction. *Agricultural Biotechnology Journal,* 18(3), 477-504.

Agricultural Biotechnology Journal, 18(3), 477-504. DOI: 10.22103/jab.2026.27154.1897

Received: March 22, 2026. Received in revised form: May 17, 2026.

Accepted: May 18, 2026. Published online: June 30, 2026.

Publisher: Shahid Bahonar University of Kerman & Iranian Biotechnology Society.

Introduction

Acute myocardial infarction (AMI) is a predominant cause of morbidity and mortality globally, mostly caused by coronary artery occlusion, which leads to myocardial ischemia and irreparable cardiomyocyte damage if reperfusion is not promptly achieved. In addition to localized ischemia injury AMI initiated a multifaceted systemic response marked by the disturbance of cardiomyocyte calcium homeostasis, the activation of innate immune pathways and the dysfunction of vascular repair processes. Disruptions in intracellular calcium management are widely acknowledged as a fundamental mechanism contributing to contractile dysfunction and myocardial damage in ischemic heart disease and heart failure (Byrne et al., 2023; Martin et al., 2024). Members of the S100 protein family are crucial to these processes. S100A1 is predominantly expressed in cardiomyocytes and serves as an EF-hand calcium binding protein that modulates excitation-contraction coupling. S100A1 engages with crucial calcium regulating proteins such as ryanodine receptor (RyR2) and the sarcoplasmic reticulum Ca^{+2}-ATPase (SERCA2a), thereby improving calcium cycling efficiency, stabilizing intracellular calcium

release and facilitating mitochondrial ATP synthesis and myocardial contractility (Kraus et al., 2009; Rohde et al., 2010). Experimental and translational studies indicate that diminished S100A1 expression in ischemic myocardium correlates with compromised calcium handling, reduced contractility and energetic dysfunction, while restoration of S100A1 levels enhances myocardial performance and recover following ischemic injury (Pleger et al., 2005; Ritterhoff & Most, 2012). Unlike the cardiomyocyte specific function of S100A1, S100A8/A9 (calprotectin) serves as a pro-inflammatory constituent of the S100 protein family, primarily secreted by activated neutrophils and monocytes during acute inflammatory responses. S100A8/A9 functions as a damage associated molecular pattern (DAMP). This activates pattern-recognition receptors, such as Toll-like receptor-4 (TLR4) and the receptor for advanced glycation end products (RAGE), thereby augmenting innate immune signaling and promoting cytokine production, leukocyte recruitment, and inflammatory damage in the infarcted myocardium (Frangogiannis et al., 2002; Zhou et al., 2023). Recent studies reveal that circulating S100A8/A9 levels are elevated in cardiovascular diseases and may serve as diagnostic or prognostic biomarkers in myocardial infarction and related ailments (Vogl et al., 2014; Martin et al., 2024). Human calprotectin is a calcium-binding heterodimer consisting of the S100A8 and S100A9 subunits, capable of forming higher-order oligomeric complexes under physiological conditions. This complex binds not only calcium but also transition metals like zinc and manganese, which enhances its antibacterial properties and regulatory function in immune responses during inflammatory situations (Zygiel & Nolan, 2019; Guan et al., 2025). Inflammatory mediators produced with cardiac damage additionally affect cardiomyocyte function. Tumor necrosis factor-α (TNF-α) is a pivotal cytokine in the innate immune response, playing a significant role in endothelial dysfunction, oxidative stress, and cardiac contractile impairment. Significantly, inflammatory cytokines can impair intracellular calcium cycling and mitochondrial function, hence associating immune activation with cardiomyocyte failure after myocardial ischemia (Obeagu, 2025; Mann, 2026). Vascular endothelial growth factor-A (VEGF-A) is essential for post-ischemic angiogenesis, endothelial survival, and microvascular repair. Decreased VEGF signaling has been linked to compromised neovascularization and adverse ventricular remodeling after myocardial infarction (Carmeliet & Jain, 2011; Florek et al., 2024). The individual functions of calcium dysregulation, inflammatory signaling, and angiogenic imbalance have been extensively researched; nevertheless, their coordinated interplay within a cohesive biological framework during acute myocardial infarction is still not fully comprehended. Recent data indicates that myocardial damage may include synchronized disruptions connecting cardiomyocyte calcium regulation with innate immune activation and compromised vascular repair mechanisms (Carmeliet & Jain, 2011; Vogl et al., 2014; Zhou et al., 2023). Moreover, the epigenome, which comprises various mechanisms such as DNA methylation, chromatin remodeling, histone tail modifications, microRNAs, and long non-coding RNAs, interacts with environmental factors like nutrition, pathogens, and climate to influence gene expression profiles and the emergence of specific phenotypes (Kazemipour et al., 2025; Mohammadabadi et al., 2023). These interactions are complex and occur across multiple levels, involving dynamic crosstalk between the genome, epigenome, and environmental stimuli (Khezri et al., 2025). Increasing evidence suggests that epigenomic variation plays a crucial role

in determining health outcomes and production traits (Alavi et al., 2022; Safaei et al., 2022). The expression of eukaryotic genes is temporally and spatially regulated through multidimensional control mechanisms (Hajalizadeh et al., 2021). Only a limited subset of the entire genome is actively expressed in each tissue type, and gene expression is closely tied to developmental stages (Mohammadabadi et al., 2025; Khabiri et al., 2025). Consequently, gene expression patterns in eukaryotes are tissue-specific (Farahvashi et al., 2026a; Mohammadabadi et al., 2024). Additionally, the levels of gene products synthesized within a given tissue, as well as those contributed by other tissues, collectively regulate gene expression (Alhasoon et al., 2026). Epigenetic modifications serve as a critical mechanism by which environmental factors leave a lasting imprint on the genome (Mohammadabadi et al., 2022a). These modifications can be heritable, influencing successive generations without altering the DNA sequence itself (Mohammadabadi et al., 2025). For instance, maternal nutrition during pregnancy has been shown to induce epigenetic changes that affect offspring metabolism, growth, and disease susceptibility (Safaei et al., 2024). Similarly, environmental stressors such as exposure to toxins or pathogens can trigger epigenetic responses that modify gene expression and cellular function (Noori et al., 2017). Understanding epigenetic mechanisms can improve breeding strategies, enhance productivity, and promote disease resistance (Roudbar et al., 2015). Additionally, epigenetic markers are increasingly used to predict performance and health outcomes, providing a valuable tool for precision (Mohamadinejad et al., 2024). A fundamental aspect of genetic research involves the investigation of genes and proteins associated with specific traits, examined at both cellular and chromosomal levels (Farahvashi et al., 2026b). Advancing our understanding of these regulatory processes holds significant potential for improving biological insights and practical applications in health and production (Arabpour et al., 2021). Further research into epigenetic biomarkers and their role in gene regulation will contribute to more effective therapeutic strategies and enhanced understanding of complex biological systems (Mohammadabadi et al., 2022b). Thus, this study aims to examine the protein and gene expression patterns of S100A1 and S100A8/A9 in patients with acute myocardial infarction, and to assess their correlation with circulating calcium levels, inflammatory signaling (TNF-α), and angiogenic activity (VEGF-A). This work aims to elucidate the relationship among calcium dysregulation, inflammatory activation, and compromised angiogenesis in the pathogenesis of acute myocardial infarction through the integration of biochemical, molecular, and statistical analysis.

Materials and methods

Study design and population: This case-control study was conducted in the laboratories of the Department of Chemistry and Biochemistry at the College of Medicine, University of Babylon, Iraq, in collaboration with Merjan Medical City and Al-Hilla Teaching Hospital, including the Surgical Specialty Hospital-Cardiac Center. Between March and May 2025, 200 consecutive adults aged 45 to 70 years were evaluated for eligibility. Participants displaying clinical or laboratory indications of acute or chronic infection were removed to mitigate any confounding effects on inflammatory biomarkers. After applying the exclusion criteria, 24

individuals were removed yielding a final study group of 176 participants, which comprised: 88 individuals diagnosed with acute myocardial infarction and 88 presumably healthy controls. Controls were matched with cases according to age and sex to maintain a 1:1 case-control ratio. Figure 1 displays the inclusion and exclusion process, whereas Figure 2 delineates the full analytical workflow of the study.

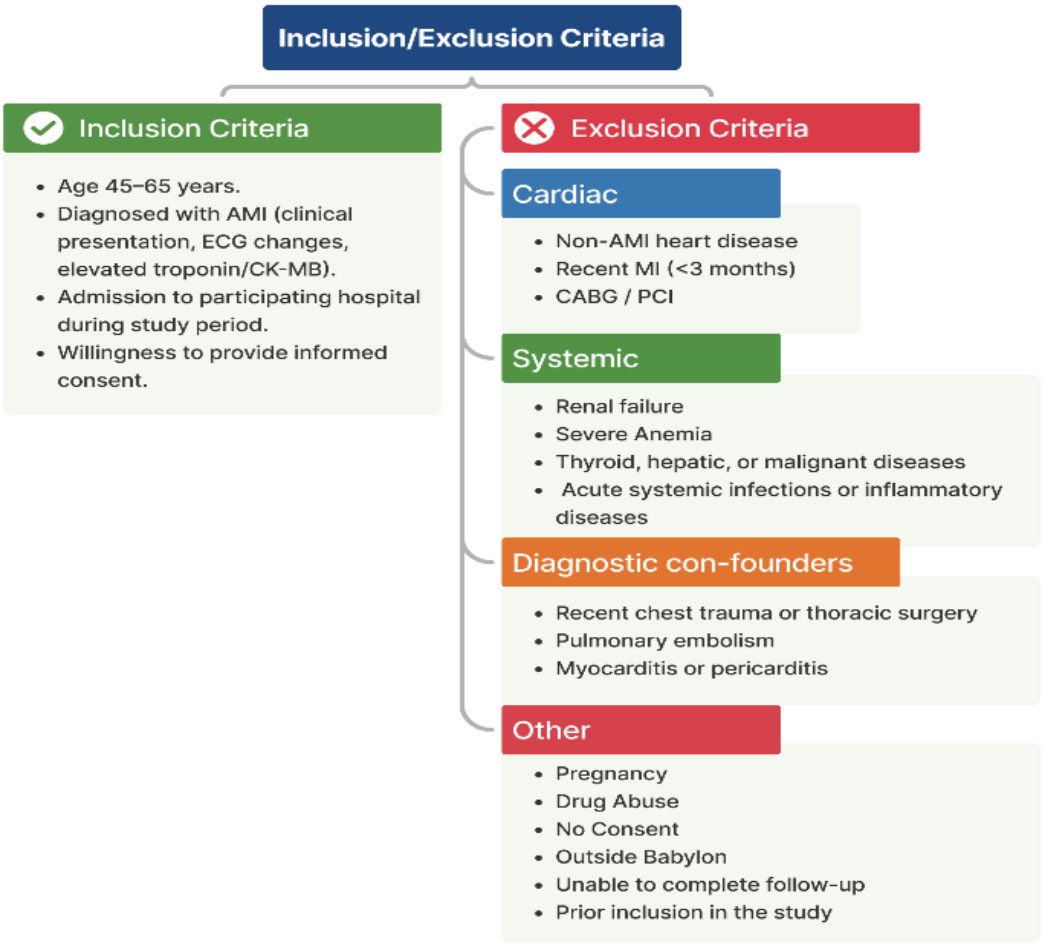

Figure 1. Flow diagram showing the screening of 200 participants, with 24 excluded due to infection, resulting in the final inclusion of 176 participants

Diagnostic criteria for acute myocardial infarction: The diagnosis of AMI was made in accordance with the Fourth Universal Definition of Myocardial Infarction, aligning with the guidelines of the European Society of Cardiology (ESC) and the American College of Cardiology/American Heart Association (ACC/AHA). The diagnostic criteria encompassed 1- existence of ischemia manifestations, 2- dynamic electrocardiographic changes compatible with myocardial ischemia, and 3- An increase or decrease in cardiac troponin levels, with at least one measurement surpassing the 99th percentile upper reference limit, is also observed.

Ethical Approval: This study was conducted in accordance with the principles of the Declaration of Helsinki (2013 version) after obtaining ethical approval from the Research Ethics

Committee at the College of Medicine, University of Babylon, Iraq, and written informed consent was obtained from all participants before joining the study.

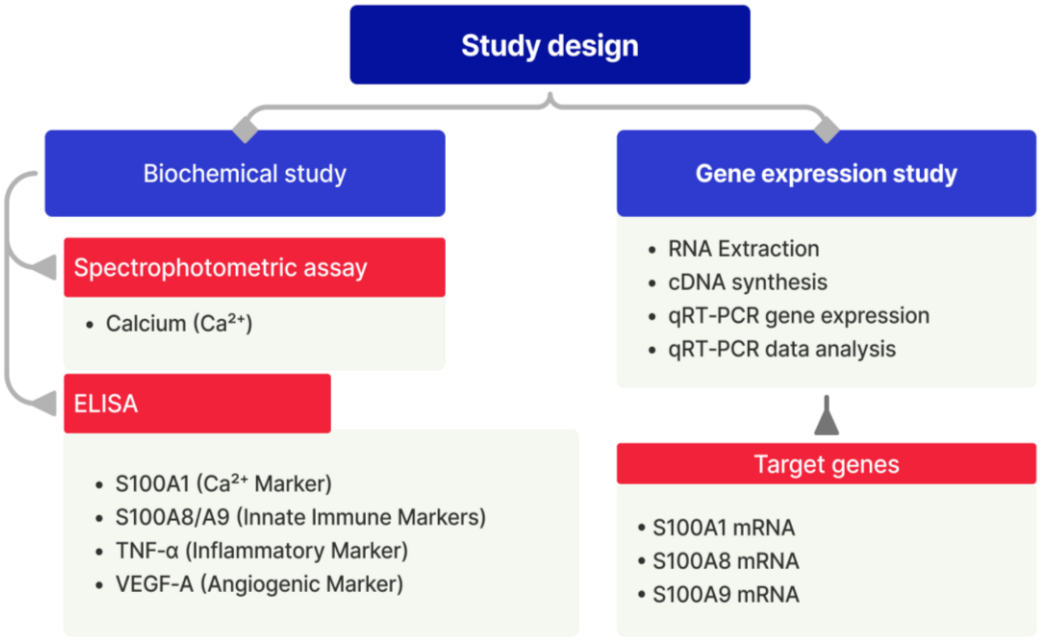

Figure 2. Schematic representation of the study design integrating biochemical and gene expression analyses

Sample size estimation: The sample size for this case-control comparative study was estimated to ensure sufficient statistical power to detect statistically significant differences in biomarker levels between patients with acute myocardial infarction and healthy individuals. The G*Power software (version 3.1) was used to perform the calculation, assuming a two-tailed significance level ($\alpha = 0.05$) and a statistical power of 80% ($1 - \beta = 0.80$), as these criteria are widely recommended in biomedical research to reduce type I and type II errors in studies comparing the means of two independent groups. The required sample size was estimated using the following equation (Faul et al., 2007; Faul et al., 2009).

$$n = \frac{(Z_B + Z_{a/2})^2 \times 2 \times SD2}{d^2}$$

Where, **n** = Minimum required sample size for each group, **d** = Expected mean difference between cases and controls, $\mathbf{Z_\beta}$ = Standard normal deviate corresponding to statistical power (for 80% power, $Z\beta = 0.84$), $\mathbf{Z_{\alpha/2}}$ = Standard normal deviate corresponding to the level of significance (for $\alpha = 0.05$, $Z\alpha/2 = 1.96$), **SD** = Standard deviation = Expected mean difference between case and control (previously published studies), and **r** = Ratio of controls to cases (r = 1 when equal numbers of cases and controls are included).

Clinical assessment: Clinical variables included age, sex, BMI, smoking status, hypertension, diabetes mellitus, and family history of cardiovascular disease.

Blood sample collection: Venous blood (5 mL) was collected aseptically from each participant under standardized conditions. Three milliliters were transferred to gel-separator tubes, allowed to clot, and centrifuged at 2000 × g for 15 minutes to obtain serum, and the separated serum was a liquoted and stored at −80°C until analysis. Two milliliters were collected into EDTA tubes and immediately snap-frozen in liquid nitrogen (−196°C) for RNA extraction. The remaining 2 mL of whole blood were collected into EDTA-containing tubes and immediately preserved in liquid nitrogen at −196°C for subsequent RNA extraction and gene expression analysis (Table 1).

Table 1. Blood Sample Collection and Processing Protocol

Sample Type	Volume	Processing
Serum	3 mL	Centrifuged at 2000×g for 15 min, stored at −38°C
Whole blood (RNA)	2 mL	Stored in liquid nitrogen (−196°C)

Table 2. Summary of Biomarker Measurement Techniques

Biomarker	Method	Technique Details
S100A1, TNF-α, VEGF-A	ELISA	Bioassay Technology Laboratory kits
S100A1, S100A8, S100A9 mRNA	qPCR	SYBR Green chemistry (GoTaq® Master Mix)
Calcium (Ca^{2+})	Spectrophotometry	O-CPC method, λ = 578 nm

Biochemical analysis: Circulating levels of S100A1 protein, S100A8/A9 complex, TNF-α, and VEGF-A were quantified using commercially available enzyme-linked immunosorbent assay (ELISA-based assays) kits according to the manufacturer's instructions. Absorbance was measured using a microplate reader, and concentrations were calculated based on the corresponding standard calibration curves generated for each biomarker.

Determination of serum calcium: For measurement of human serum calcium, the spectrophotometer device was supplied with a kit provided by Fuji Xerox Co. (China). Serum calcium levels were checked using a color test with o-cresolphthalein complexone (O-CPC) on a Spectrum spectrophotometer set to 578 nm and a 1-cm light. The assay was performed at room temperature using an endpoint method with a reagent blank for zero adjustment. The ratio of sample to reagent was maintained at 1:100, and calcium concentrations were calculated using the manufacturer-provided calibration standards.

RNA extraction and quantitative Real-Time PCR (qRT-PCR): Total RNA extraction from fresh whole blood samples was performed according to the manufacturer's protocol (Favorgen Biotech Corp., Taiwan). The concentration and purity of extracted RNA determined by using the Nano Drop spectrophotometer. Only RNA samples with adequate purity ratios (A260/A280 = 1.8-2.1) were used for subsequent analyses (Bustin et al., 2009; Taylor et al., 2019; Bustin, 2025). Samples with enough purity ratios were utilized for complementary DNA (cDNA) synthesis and subsequent quantitative real-time PCR (qRT-PCR) analysis, whereas samples with insufficient purity were reassessed before further processing (Postollec et al., 2011). cDNA was synthesized using the GoTaq® 1-Step RT-qPCR System according to the manufacturer's

protocol. The reverse transcription reaction was conducted in a total volume of 20 µL, comprising an RNA template, an RT reaction premix with oligo(dT) and random primers, a FIRE Script enzyme mix, and nuclease-free water (Table 3). The reaction mixture was gently agitated, briefly centrifuged, and underwent reverse transcription according to the thermal profile detailed in Table 4, which included primer annealing at 25°C for 5-10 minutes, reverse transcription at 37-60°C for 15-30 minutes, and enzyme inactivation at 85°C for 5 minutes (Figure 3). The generated cDNA was either utilized immediately for qRT-PCR amplification of the *S100A1, S100A8,* and *S100A9* genes or preserved at −20 °C for future investigation. Gene expression levels were quantified using the $2^{-\Delta\Delta Ct}$ method, with GAPDH used as the internal reference gene.

Table 3. Composition and final concentrations of the reverse transcription reaction mixture

Component	Volume	Final concentration
DNase/RNase free water	Up to 20 µL	Variable
RT reaction premix with oligo (dT) and 10X random primers	2 µL	1X
RNA template	0.1-5 ng	Variable
FIRE Script enzyme mix solution	1.5 µL	
Total reaction volume	20 µL	

Table 4. Thermal cycling conditions for reverse transcription reaction

Step	Temperature	Time
Primer annealing	25 °C	5-10 min
Reverse transcription	37-60 °C	15-30 min
Enzyme inactivation	85 °C	5 min

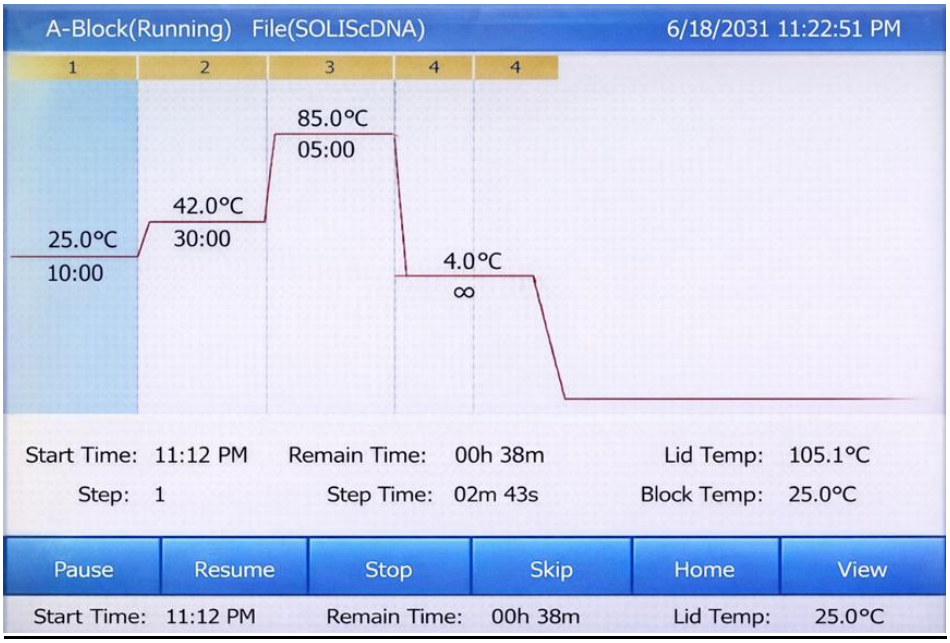

Figure 3. Thermal profile of the Reverse Transcription (cDNA synthesis) protocol

Relative expression of S100A1, S100A8, and S100A9 mRNA in AMI: Gene expression analysis of the S100A1, S100A8, and S100A9 target genes was performed. Glyceraldehyde-3-phosphate dehydrogenase (GAPDH) was used as the endogenous reference gene for normalization of expression levels.

Primer design and validation: Quantitative polymerase chain reaction (qPCR) was performed using primers specifically designed to amplify the S100A1, S100A8, and S100A9 genes. Primer sequences were selected from well-documented published data and confirmed to match the target transcripts. The GAPDH gene was used as an internal reference gene to standardize gene expression levels. Primers for the S100A1, S100A8, S100A9, and GAPDH genes were commercially manufactured by ORIGENE, USA. The primer sequences and amplification product characteristics are listed in Table 5.

Table 5. Primer sequences used in qRT-PCR analysis

Gene	Primer name	Sequence (5′→3′)	Product Size (bp)	Accession No
S100A1	F	GTACAAGCTGAGCAAGAAGGAGC	115 bp	NM_006271
	R	CTCGTCTAGCTCCTTCATCACC		
S100A8	F	ATGCCGTCTACAGGGATGACCT	142 bp	NM_002964
	R	AGAATGAGGAACTCCTGGAAGTTA		
S100A9	F	GCACCCAGACACCCTGAACCA	124 bp	NM_002965
	R	TGTGTCCAGGTCCTCCATGATG		
GAPDH	F	GGAGTCAACGGATTTGGT	206 bp	NM_002046.7
	R	GTGATGGGATTTCCATTGAT		

All primers were freeze-dried. According to the manufacturer's instructions, each primer was mixed with nuclease-free double-distilled water (ddH_2O) to prepare a basic solution with a final concentration of 100 pmol/µL. To prevent repeated freezing and thawing of the basic solutions, they were divided into smaller quantities and stored at -20°C. A working solution of 10 pmol/µL was prepared for standard polymerase chain reaction (PCR) experiments by mixing the basic solution with nuclease-free double-distilled water.

Quantification Real-Time polymerase chain reaction (qRT-PCR): Gene expression analysis was performed using an Agilent Mx3005P Real-Time PCR system (Agilent Technologies, Santa Clara, CA, USA). Reverse transcription and quantitative DNA amplification (qPCR) were performed in one step using a GoTaq® 1-Step RT-qPCR system (Promega, Madison, WI, USA), according to the manufacturer's instructions. Each reaction was performed in a final volume of 20 µL containing GoTaq® qPCR Master Mix, Go Script™ RT Mix for 1-Step RT-qPCR, gene-specific forward and reverse primers (at final concentrations of 0.2-0.4 µM each), RNA template, and nuclease-free water. The reaction was performed in a final volume of 20 µL containing GoTaq® qPCR Master Mix, Go Script™ RT Mix for 1-Step RT-qPCR, gene-specific forward and reverse primers (at final concentrations of 0.2-0.4 µM each), RNA template, and nuclease-free water. The thermal cycling conditions were as follows: reverse transcription at

37°C for 15 min, followed by initial denaturation at 95°C for 10 min, and then 40 amplification cycles consisting of denaturation at 95°C for 15 s and annealing/elongation at 60°C for 60 s. Fluorescence data were obtained during the elongation phase of each cycle using SYBR® Green detection technology. Amplification curves and cycle threshold (Ct) values were analyzed using MxPro qPCR software (Agilent Technologies, USA).

Protocol for the GoTaq® 1-Step RT-qPCR system for Real-Time qPCR (gene expression assay) utilized for the quantification of S100A1, S100A8, S100A9, and GAPDH (housekeeping gene) Expression- Assembling the reaction mixture (20 µL total volume): The reaction mixes by combining GoTaq® qPCR master mix, nuclease-free water and primers were prepared as showed in Table 6.

Table 6. Preparation of Real-Time PCR reactions

Components	Concentration	Volume (20 µL)
GoTaq® qPCR Master Mix (2X)	1X	10 µL
Forward primer (20X)	10 µM/µL	2 µL
Reverse primer (20X)	10 µM/µL	2 µL
ddH_2O	-	4 µL

Then, 18 µL of reaction mix was carefully placed into each reaction tube and was add 2 µL of cDNA template (10-100 ng), standard or negative control to each tube and final volume became 20 µL. The tubes were sealed for 1 minute, mixed by overtaxing briefly to collect the contents of the tubes at the bottom, and the samples are ready for thermal cycling (Table 7).

Table 7. qPCR thermal cycling conditions using GoTaq® hot start polymerase

Stage	Ta (°C)	Time	Cycles
GoTaq® Hot Start Polymerase activation (initial activation)	95	2 min	1
Denaturation	95	15 sec.	40X
Annealing/data collection/extension with fluorescence acquisition	60	1 min	

After performing qPCR, achieved results were analyzed. The melt curve analysis revealed the specificity of amplification by indicating a distinct sharp peak for each gene product. This signified the lack of primer-dimers and non-specific amplification. Each run features controls that do not employ templates for contamination detection. The comparative threshold cycle method (2^−ΔΔCt) was used to assess the relative expression levels of the S100A1, S100A8, and S100A9 genes. Then data was analyzed and was compared with those of the control group. The threshold cycle (Ct) values were independently calculated using instrument's software. All procedures complied with the Minimum Information for Publication of Quantitative Real-Time PCR Experiments (MIQE) criteria to guarantee the accuracy and reproducibility of the results (Bustin et al., 2009; Taylor et al., 2019) (Figure 4).

Relative gene expression analysis: Relative gene expression levels of *S100A1, S100A8*, and *S100A9* were quantified using the comparative threshold cycle (2^−ΔΔCt) method. In this

approach, the cycle threshold (Ct) values of the target genes were first normalized to the internal reference gene GAPDH to obtain the ΔCt value for each sample.

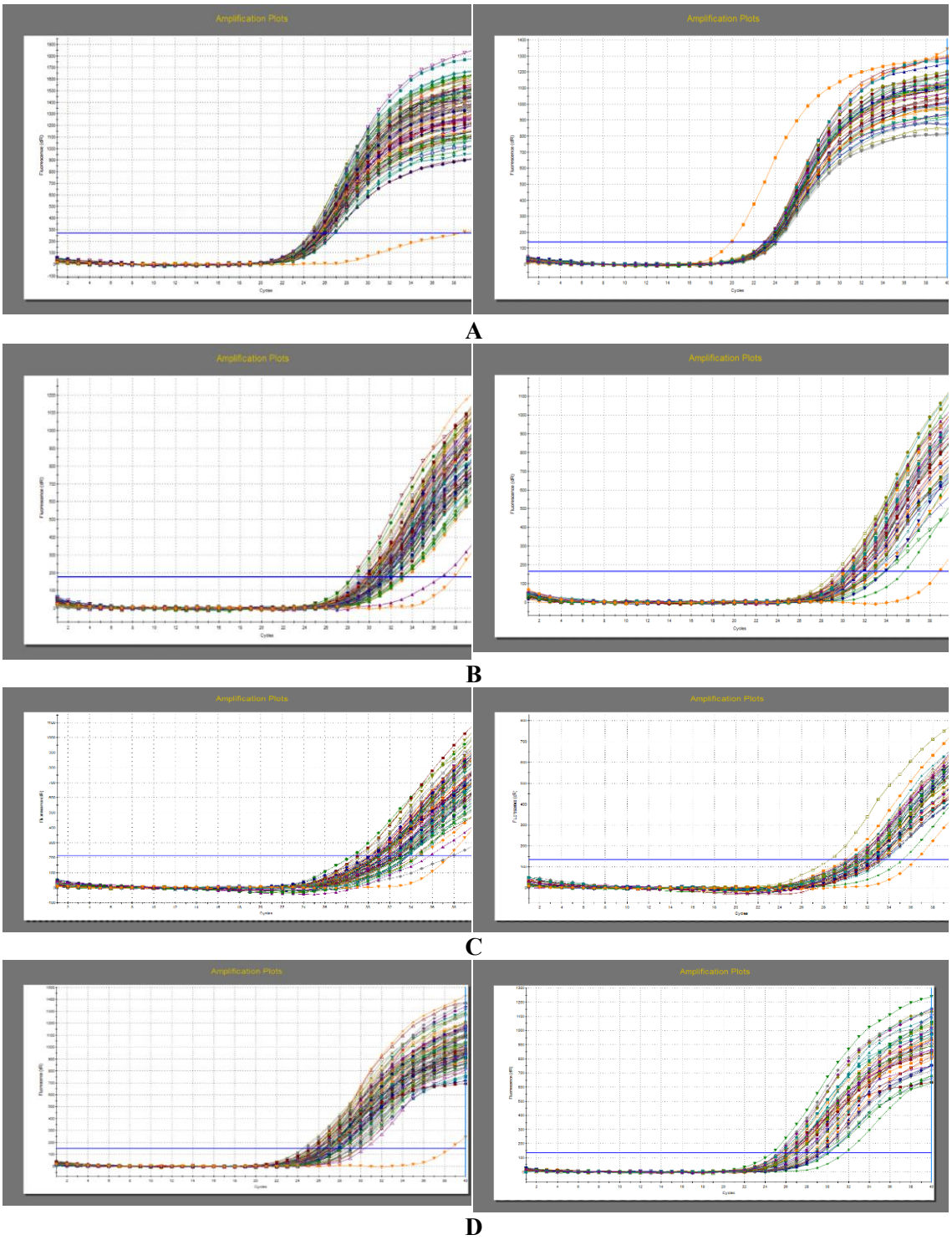

Figure 4. Amplification curves for (A) S100A1, (B) S100A8, (C) S100A9, and (D) the housekeeping gene (GAPDH) showing delayed Ct values in AMI patients compared to controls

Subsequently, the ΔCt values of the patient samples were compared with those of the control group to calculate the ΔΔCt values. The relative fold change in gene expression was then determined using below equation:

$$\textbf{Fold Change} = 2^{-\Delta\Delta Ct}$$

Where, ΔCt = Ct (target gene) − Ct (reference gene), and ΔΔCt = ΔCt(sample) − ΔCt(control). This method enables the determination of relative differences in gene expression between experimental groups. It is widely used for quantitative analysis of gene expression in real-time PCR experiments (Bustin et al., 2009; Taylor & Mrkusich, 2014).

Results

Clinical characteristics: No significant differences were observed in age or sex distribution between groups ($p > 0.05$), confirming appropriate matching. Significant associations with AMI were observed for hypertension (OR = 3.58, $p < 0.001$), diabetes mellitus (OR = 2.20, $p = 0.010$), smoking (OR = 2.16, $p = 0.015$), family history (OR = 2.13, $p = 0.014$), and overweight status (OR = 1.92, $p = 0.041$) (Table 8).

Table 8. Baseline clinical characteristics and risk factors in AMI patients and controls

Variable	AMI patients (n = 88)	Controls (n = 88)	OR (95% CI)	P-value
Age (years) mean ± SD	58.52 ± 8.58	56.68 ± 9.02	1.02 (0.99-1.06)	0.125
	Sex			
Male, n (%)	48 (54.5%)	48 (54.5%)	1.00 (0.55 - 1.82)	1.000
Female, n (%)	40 (45.5%)	40 (45.5%)		
	BMI category			
Normal weight	50 (56.8%)	63 (71.6%)	1.92 (1.02 - 3.60)	0.041
Overweight	38 (43.2%)	25 (28.4%)		
	Family history of CVD			
Yes	45 (51.1%)	29 (33.0%)	2.13 (1.16 - 3.90)	0.014
No	43 (48.9%)	59 (67.0%)		
	Smoking			0.015
Yes	30 (34.1%)	17 (19.3%)	2.16 (1.09 - 4.27)	
No	58 (65.9%)	71(80.7 %)		
	Hypertension			
Yes	54 (61.4%)	27 (30.7%)	3.58 (1.92 - 6.67)	<0.001
No	34 (38.6%)	61 (69.3%)		
	Diabetes mellitus			
Yes	49 (55.7%)	32 (36.4%)	2.20 (1.20 - 4.02)	0.010
No	39 (44.3%)	56 63.6%)		

ROC analysis: To identify independent predictors of acute myocardial infarction, multivariate logistic regression analysis was performed including clinical variables and molecular

biomarkers. As shown in Table 2, S100A1 and serum calcium emerged as significant independent predictors of AMI after adjustment for confounding factors. In contrast, TNF-α did not demonstrate independent predictive value, consistent with its poor diagnostic performance in ROC analysis. S100A1 retained its significance after adjustment, supporting its role as a primary marker of cardiomyocyte dysfunction rather than a secondary inflammatory response. These findings reinforce the hierarchical model in which calcium dysregulation precedes inflammatory activation and angiogenic impairment in AMI.

Multivariate logistic regression analysis: Biochemical and protein biomarkers demonstrated distinct diagnostic and predictive characteristics for acute myocardial infarction (AMI), as summarized in (Table 9). Serum calcium exhibited good diagnostic performance (AUC=0.82, 95% CI: 0.75-0.88), with high specificity (88.6%), supporting its role as a reliable indicator of disrupted calcium homeostasis. Among protein biomarkers, S100A1 showed a moderate AUC (0.69) but achieved perfect specificity (100%), indicating strong rule-in potential despite relatively limited sensitivity. S100A8/A9 demonstrated acceptable diagnostic performance (AUC=0.76), consistent with its role as a marker of inflammatory activation. In contrast, TNF-α showed no significant discriminatory ability (AUC=0.50), while VEGF exhibited poor diagnostic performance (AUC=0.54), suggesting limited utility as standalone diagnostic markers. To further determine whether these biomarkers represent independent predictors of AMI, multivariate [logistic regression analysis was performed including biochemical, molecular and clinical variables. As shown in Table 2, serum calcium and S100A1 remained significant independent predictors after adjustment for potential confounders, whereas TNF-α did not demonstrate independent predictive value, consistent with its lack of diagnostic discrimination in ROC analysis.

Table 9. Diagnostic performance of biochemical and protein biomarkers in AMI (ROC analysis)

Category	Biomarker	AUC	95% CI	Sensitivity (%)	Specificity (%)	Interpretation
Biochemical	S. Calcium	0.82	0.75-0.88	62.5	88.6	Good
Protein Biomarkers	S100A1	0.69	0.47-0.90	46.2	100.0	High specificity
	S100A8/A9	0.76	0.68-0.83	70.0	72.0	Acceptable
	TNF-α	0.50	0.26-0.73	23.1	90.9	No discrimination
	VEGF	0.54	0.30-0.77	69.2	54.5	Poor

Although S100A8/A9 showed moderate diagnostic performance, its predictive effect was attenuated in multivariate model, suggesting that its contribution is partially mediated by the broader inflammatory response rather than representing a primary driver of disease. These findings are consistent with the biomarker distribution patterns illustrated in (Figure 5), which demonstrate coordinated alterations across calcium, inflammatory and angiogenic domains. Specifically, elevated calcium levels and reduced S100A1 reflect early disruption of calcium-regulatory mechanisms, whereas increased S100A8/A9 and TNF-α indicate activation of

inflammatory pathways. Concurrently, decreased VEGF levels suggest impaired angiogenic signaling.

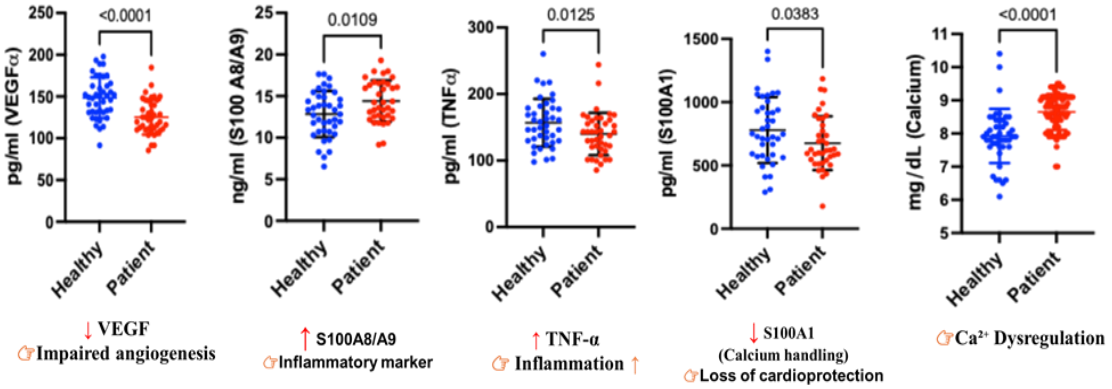

Figure 5. Disruption of the calcium-inflammation-angiogenesis axis in acute myocardial infarction

The ROC curve, multivariate adjusted predictive analysis, and biomarker distribution patterns support a hierarchical model of pathophysiological disturbance in acute myocardial infarction. This model suggests that calcium-induced changes represent a primary event, followed by secondary inflammatory activation, and subsequently, angiogenesis signaling dysfunction. In this context, the continued independent predictor of S100A1 after multivariate adjustment reinforces its role as a primary marker of myocardial dysfunction, rather than a secondary consequence of systemic inflammation.

Molecular biomarkers: Analysis of gene expression levels further supported these findings, as summarized in (Table 10). *S100A1* mRNA expression was markedly downregulated in AMI patients compared to healthy controls (median: 2.45 vs. 11.47, p<0.0001), indicating a substantial disruption in calcium-regulatory pathways. Conversely, *S100A8* and *S100A9* mRNA levels were significantly upregulated in patients (S100A8: p=0.030; S100A9: p=0.044), reflecting activation of inflammatory signaling (Figure 6).

Table 10. Gene expression levels of S100 family biomarkers in AMI patients and healthy controls

Gene (mRNA expression)	Group	Median (IQR)	Min-Max	Mean ± SD	95% CI	P-value
S100A1	Healthy	11.47 (5.94-28.84)	2.67-90.51	21.47 ± 22.66	14.81-28.12	
	Patients	2.45 (1.33-4.09)	0.41-18.00	3.35 ± 2.99	2.72-3.97	<0.0001
S100A8	Healthy	0.060 (0.029-0.104)	0.008-0.192	0.072 ± 0.049	0.057-0.087	0.030
	Patients	0.071 (0.049-0.115)	0.012-0.717	0.114 ± 0.119	0.087-0.140	
S100A9	Healthy	0.034 (0.019-0.051)	0.006-0.120	0.041 ± 0.028	0.032-0.049	0.044
	Patients	0.040 (0.023-0.075)	0.010-0.524	0.070 ± 0.091	0.050-0.090	

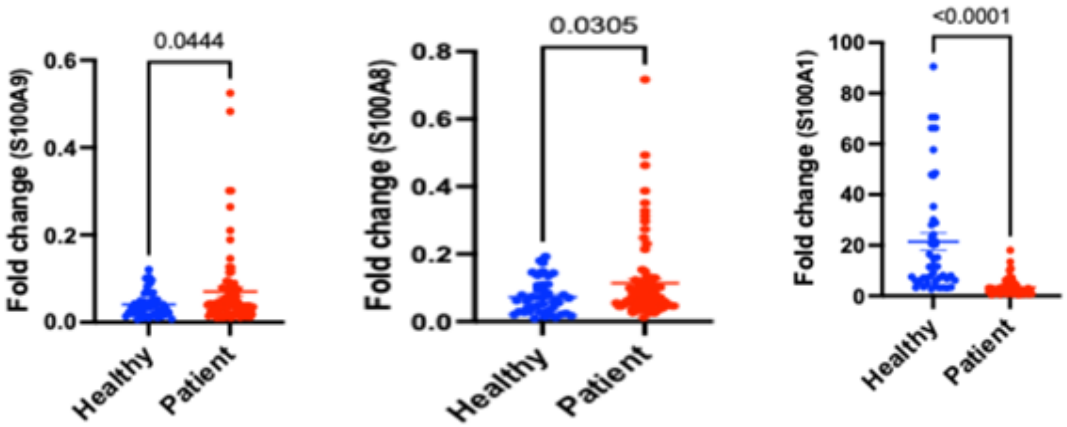

Figure 6. Differential expression of S100 family biomarkers in AMI patients vs. healthy controls

Correlation analysis of calcium, inflammatory, and angiogenic biomarkers: Correlational analysis was performed to investigate the interrelationships among calcium-regulatory, inflammatory and angiogenic biomarkers in patients with acute myocardial infarction (AMI). The results are shown in Figure 7.

Figure 7. Correlational matrix of calcium, inflammatory and angiogenic biomarkers in acute myocardial infarction

The correlation matrix revealed a strong association between *S100A8* and *S100A9* mRNA expression (r=0.80, p<0.001), indicating coordinated activation of inflammatory pathways. In contrast, *S100A1* mRNA showed no significant correlation with inflammatory markers, supporting its independent role in cardiomyocyte calcium regulation. A significant negative correlation was observed between serum calcium and VEGF-A (r= -0.39, p= 0.035), suggesting a link between calcium dysregulation and impaired angiogenic signaling.

Statistical analyses: Statistical analyses were performed using IBM SPSS Statistics version 25.0 (IBM Corp., Armonk, NY, USA) and Graph Pad Prism version 10 (Graph Pad Software, San Diego, CA, USA). Sample size was estimated a priori using G*Power software (version 3.1) based on a significance level of $\alpha = 0.05$, statistical power of 80%, and a moderate effect size (Cohen's $d = 0.50$), according to standard power analysis procedures described by Faull et al. (2007). Continuous variables were assessed for normality using the Shapiro-Wilk and Kolmogorov-Smirnov tests. Normally distributed data are presented as mean ± standard deviation (SD), whereas non-normally distributed variables are expressed as median with interquartile range (IQR). Categorical variables are presented as frequencies and percentages. Comparisons between two independent groups (acute myocardial infarction vs. control) were performed using the independent-samples t-test for normally distributed variables and the Mann-Whitney U test for non-parametric variables. Associations between categorical variables were analyzed using the Chi-square test or Fisher's exact test, where appropriate. Correlation analyses were conducted using Pearson's correlation coefficient for normally distributed variables and Spearman's rank correlation coefficient for non-parametric variables. Relative mRNA expression levels of the target genes (S100A1, S100A8, and S100A9) were quantified using the $2^{-\Delta\Delta Ct}$ method, with GAPDH as the endogenous reference gene, in accordance with MIQE guidelines to ensure qPCR reliability and reproducibility. The diagnostic performance of clinical variables, biochemical parameters, and molecular biomarkers was evaluated using receiver operating characteristic (ROC) curve analysis. The area under the curve (AUC) was calculated with 95% confidence intervals (CI) to assess discriminative ability. Optimal cut-off values were determined using the Youden index, and corresponding sensitivity, specificity, positive predictive value (PPV), and negative predictive value (NPV) were reported. To assess the independent predictive value of biomarkers for acute myocardial infarction, univariate and multivariate logistic regression analyses were performed, and results were expressed as odds ratios (ORs) with 95% confidence intervals. Effect sizes for continuous variables were calculated using Cohen's d. All statistical tests were two-tailed, and a p-value < 0.05 was considered statistically significant. All analyses were conducted in accordance with recommended statistical reporting standards for biomedical research.

Discussion

The present study provides compelling and convergent evidence supporting the existence of an integrated calcium-inflammation-angiogenesis axis in the pathophysiology of AMI. The observed downregulation of S100A1 expression, coupled with elevated inflammatory mediators (TNF-α and S100A8/A9) and reduced VEGF-A levels, reflects a coordinated disruption spanning cardiomyocyte function, innate immune activation, and vascular repair capacity. Collectively, these findings align with contemporary paradigms emphasizing multi-pathway interactions in myocardial injury and post-ischemic remodeling (Frangogiannis, 2015). From a mechanistic perspective, the reduction of S100A1 is particularly significant given its established role as a key regulator of intracellular calcium homeostasis in cardiomyocytes. Through modulation of SERCA2a activity and RyR2 functions, S100A1 critically maintains excitation-contraction

coupling and mitochondrial energetics. Its downregulation, therefore, likely contributes to impaired calcium cycling, reduced contractile efficiency, and energetic failure during acute ischemic stress (Rohde et al., 2010; Duarte-Costa et al., 2014) (Figure 8).

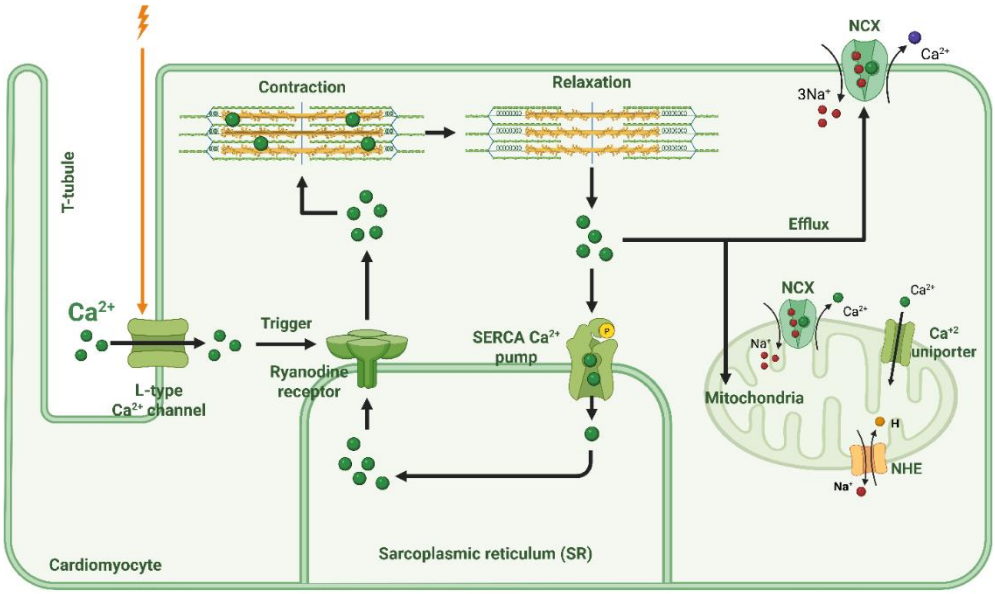

Figure 8. Mechanistic pathways underlying calcium dysregulation in acute myocardial infarction. Created in BioRender

Experimental evidence further supports this interpretation, demonstrating that S100A1 deficiency exacerbates cardiac dysfunction, whereas its restoration improves calcium handling and myocardial performance (Kehr et al., 2025; Petersen & Pepine, 2025). The present findings suggest that this calcium dysregulation occurs in parallel yet only partially interacts with inflammatory signaling pathways, indicating limited direct molecular coupling between these axes (Frangogiannis, 2015; Petersen & Pepine, 2025). In contrast, the marked elevation of S100A8/A9 reflects robust activation of the innate immune response. As a heterodimeric alarmin predominantly released by activated neutrophils and monocytes, S100A8/A9 amplifies inflammation through engagement of pattern recognition receptors, including TLR4 and RAGE, leading to NF-kB activation and downstream cytokine production (Chen et al., 2024; Sun et al., 2024) (Figure 9). This inflammatory cascade is further reinforced by increased TNF-α levels, supporting the existence of a self-propagating inflammatory loop that contributes to myocardial injury and adverse remodeling (Frangogiannis, 2015; Ma et al., 2024) (Figure 10). Recent high-impact evidence has shown that circulating S100A8/A9 is not only a strong independent predictor of post-AMI heart failure, but it may also play a role in its development. It does better than traditional biomarkers like troponin and natriuretic peptides in risk stratification models (Ma et al., 2024). These observations provide strong external validation for the current findings and highlight the active pathogenic role of S100A8/A9 beyond that of a passive inflammatory marker. Within this framework, the absence of a strong correlation between S100A1 and inflammatory mediators becomes mechanistically informative. It supports the concept that cardiomyocyte

calcium dysregulation (S100A1 axis) and systemic inflammatory activation (S100A8/A9-TNF-α axis) represent parallel yet partially interacting pathways contributing to myocardial injury.

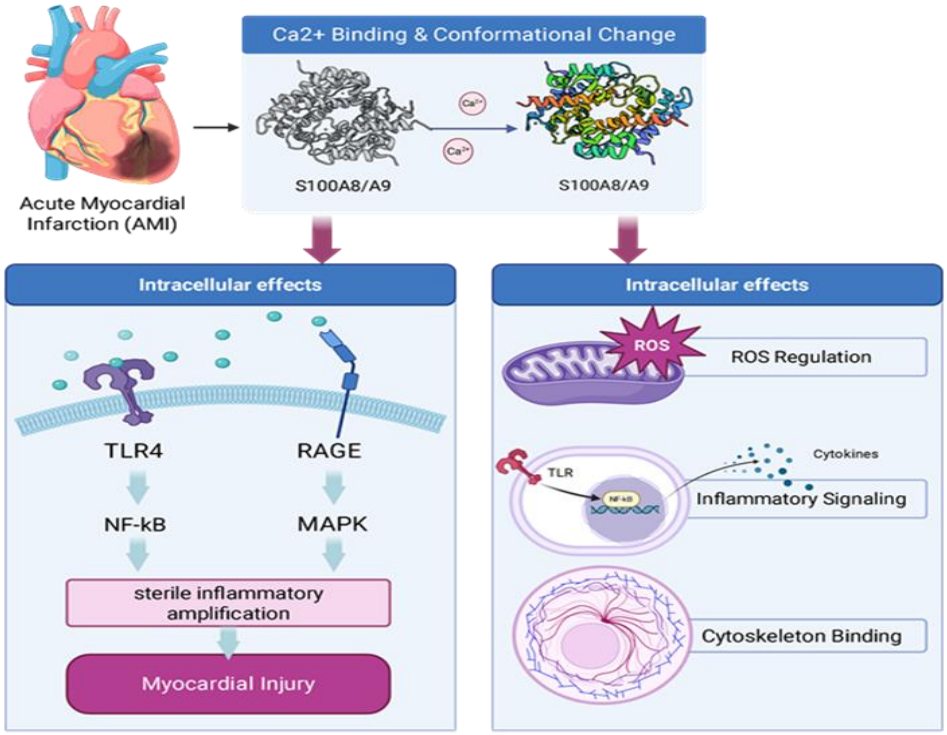

Figure 9. S100A8/A9-Mediated Crosstalk Between Calcium Signaling, Oxidative Stress, and Innate Immunity in Acute Myocardial Injury.

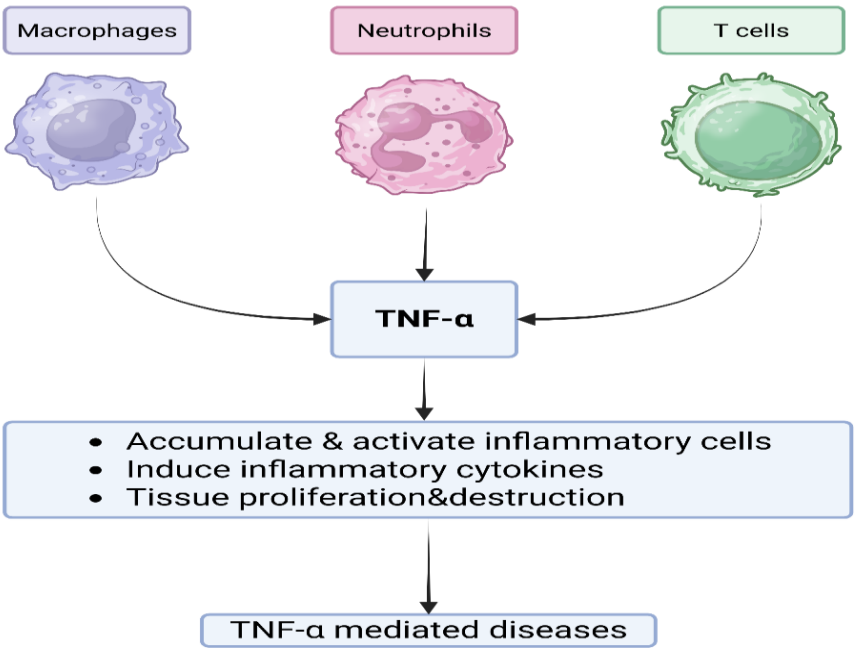

Figure 10. TNF-α-Mediated Inflammatory Activation in Acute Myocardial Infarction

The convergence of these axes likely determines the overall severity of cardiac dysfunction and clinical outcome. Furthermore, the observed reduction in VEGF-A levels indicates impaired angiogenic signaling, which may exacerbate ischemic damage by limiting endothelial repair and microvascular integrity. VEGF-A plays a pivotal role in endothelial cell survival, vascular permeability, and post-ischemic neovascularization, and its suppression has been associated with poor cardiac recovery (Deveza et al., 2012; Blake & Ridker, 2002) (Figure 11).

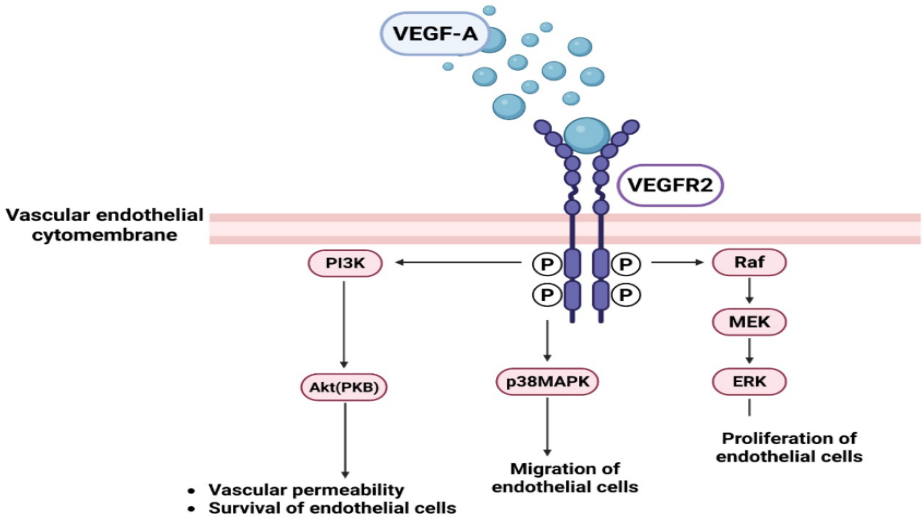

Figure 11. Molecular Mechanisms of VEGF-A-VEGFR-2 Signaling in Endothelial Activation and Angiogenesis

Excessive inflammatory activation, particularly through S100A8/A9-mediated pathways, may contribute to a maladaptive microenvironment that inhibits effective angiogenesis and delays tissue repair (Deveza et al., 2012; Duarte-Costa et al., 2014). These findings can be integrated within a hierarchical framework: primary intracellular dysfunction driven by calcium dysregulation (S100A1 axis), followed by secondary innate immune activation mediated by S100A8/A9 and TNF-α, and ultimately impaired vascular repair reflected by reduced VEGF-A levels. This sequence suggests a coordinated progression from cellular dysfunction to systemic inflammation and compromised tissue regeneration (Figure 12). From a translational perspective, the integration of these biomarkers into a unified panel offers a multidimensional assessment of myocardial injury. While S100A1 reflects cardiomyocyte functional integrity, S100A8/A9 and TNF-α capture inflammatory burden, and VEGF-A represents angiogenic capacity. This multi-axis approach may provide superior diagnostic and prognostic value compared with conventional single-marker strategies and aligns with emerging systems biology approaches in cardiovascular medicine (Taylor et al., 2014; Frangogiannis, 2015) (Figure 13).

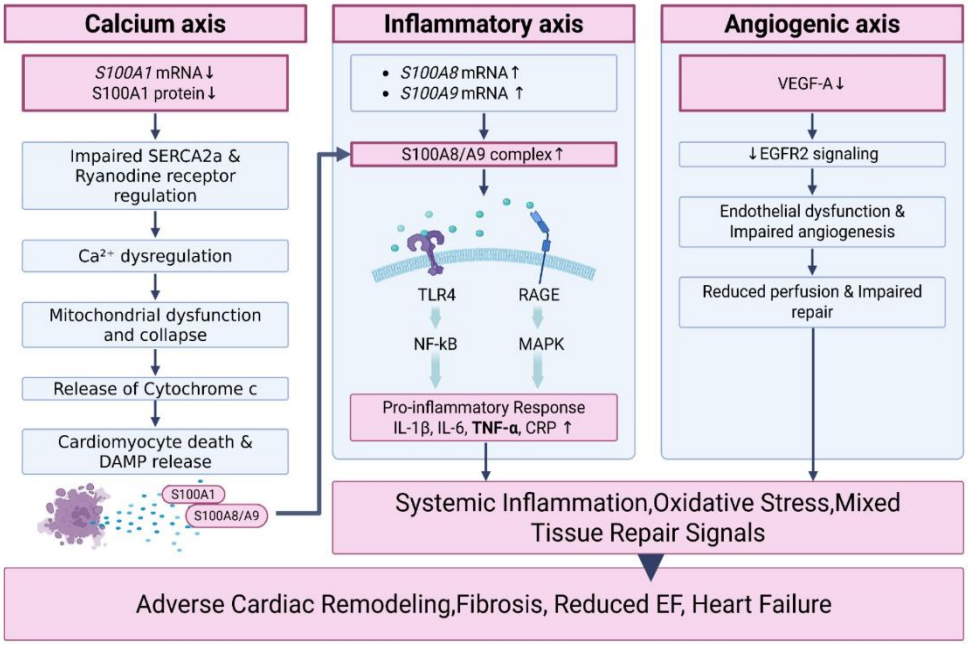

Figure 12. Integrated calcium-inflammation-angiogenesis axis driving endothelial dysfunction in acute myocardial infarction

Clinically, these findings highlight several potential implications. Adding S100A8/A9 to biomarker panels may help identify people who are at higher risk of having complications after an AMI, especially heart failure (Blake et al., 2002). Targeting inflammatory pathways such as TLR4/RAGE/NF-kB may represent a promising therapeutic strategy to attenuate inflammation-driven myocardial damage (Deveza et al., 2912; Ma et al., 2024). In parallel, restoration of S100A1 function may offer a novel approach to improving calcium handling and cardiac performance, representing a potential therapeutic target in ischemic heart disease (Duarte-Costa et al., 2014; Kehr et al., 2025). Importantly, despite the growing body of literature on individual biomarkers, few studies have simultaneously integrated calcium-regulatory proteins, inflammatory alarmins, and angiogenic mediators within a unified mechanistic framework. The present study addresses this gap and provides a comprehensive model that captures the complex, multi-dimensional nature of myocardial injury in AMI.

Study limitations: This study had several limitations. These included the exclusion of some patients due to insufficient data; all data were from a single center (Babylon Governorate), limiting the generalizability of the results; difficulty in recruiting patients due to their fear of blood draws; and the absence of detailed clinical outcome measures, such as comorbidities, which limited the correlation of results with biochemical parameters. Furthermore, environmental and lifestyle factors were not assessed. Therefore, future studies should include larger patient cohorts from multiple centers, with comprehensive clinical and biochemical assessments, as well as lifestyle evaluations, to enhance the validity and applicability of the findings.

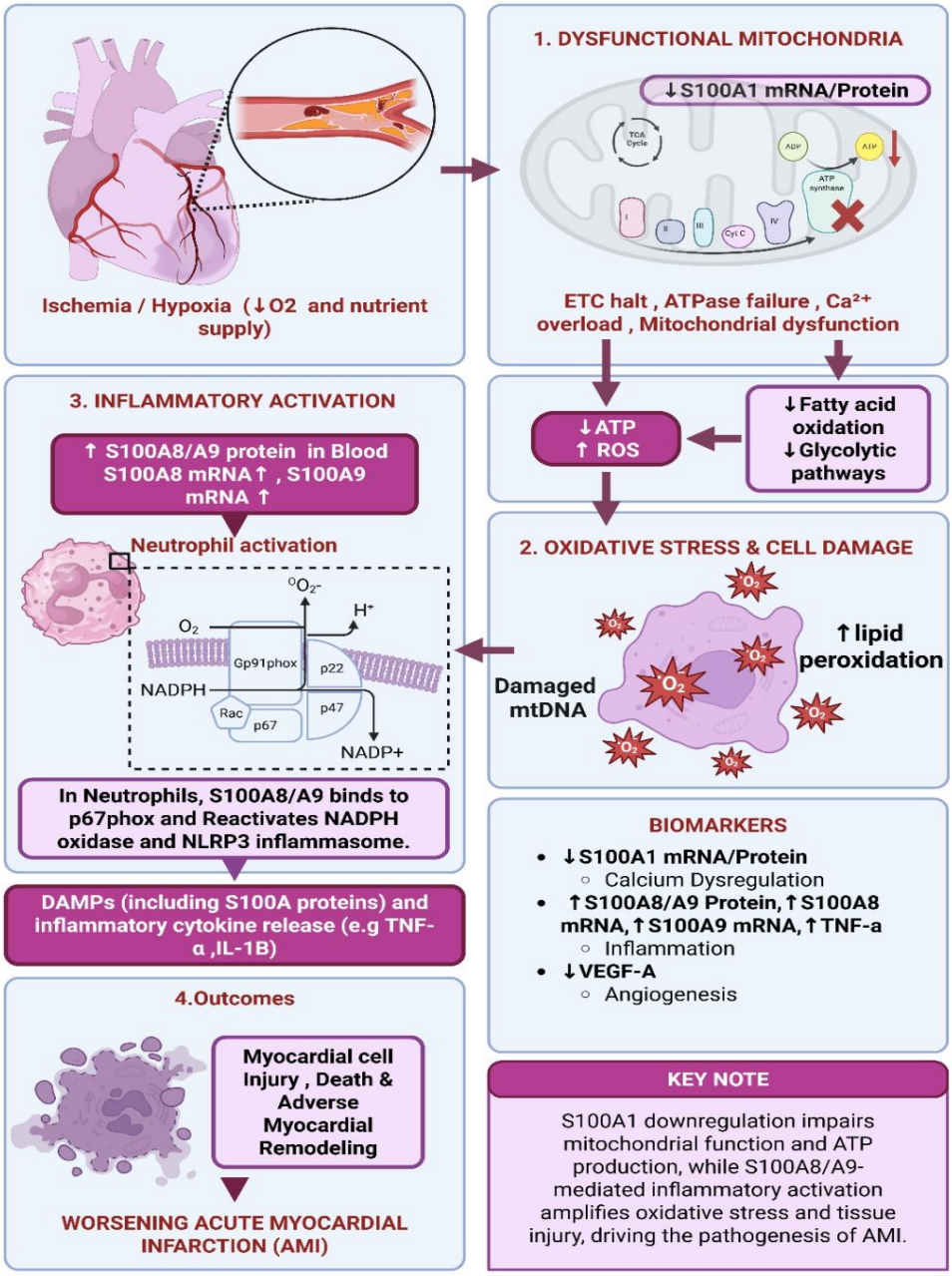

Figure 13. The Calcium-Inflammation-Mitochondrial Dysfunction Axis in Acute Myocardial Infarction (AMI)

Conclusion: AMI is not simply a case of ischemia but rather a failure of synchronization in calcium signaling, inflammatory activation, and vascular adaptation. The results of this study identified the S100A1 protein as a pivotal component of this disruption. The marked decrease in S100A1 protein levels, both at the protein and messenger RNA (mRNA) levels, indicates impaired calcium-energy coupling in cardiomyocytes at peak metabolic demand. Importantly, this deficiency appears to be biologically independent of NF-κB-dependent cytokine amplification and VEGF-A responses, suggesting that contractile dysfunction, inflammation, and

repair are mechanistically parallel rather than linearly linked processes within this model. Therefore, S100A1 is a molecular marker of myocardial energy flexibility and a potential target for therapeutic intervention in ischemic heart disease.

Authors contributions

Conceptualization: A. H. A. and A. A., Methodology: A. A. and E. F. H., Data collection and analysis: A. H. A., A. A., and E. F. H., Manuscript preparation E. F. H. and A. H. A.

Acknowledgements

The authors express their sincere appreciation to all individuals who contributed to the completion of this work. Special thanks are extended to the heart center team at Merjan Medical City (M.M.C.) for their valuable assistance in data collection and to the Department of Chemistry and Biochemistry, College of Medicine, University of Babylon, for their continuous support.

Funding

This research is supported by the Department of Clinical Biochemistry, Hammurabi College of Medicine, Babylon, University, Hillah, Iraq and self-funding. This study did not receive any external funding.

Data availability statement

The datasets used and/or analyzed during the current study are available from the corresponding author on reasonable request.

Ethical considerations

This study was conducted in accordance with the principles of the Declaration of Helsinki (2013 version) after obtaining ethical approval from the Research Ethics Committee at the College of Medicine, University of Babylon, Iraq, and written informed consent was obtained from all participants before joining the study.

Conflict of Interest

The authors declare no conflict of interest.

References

Alavi, M., Mozafari, M. R., Ghaemi, S., Ashengroph, M., Hasanzadeh Davarani, F., & Mohammadabadi, M. (2022). Interaction of epigallocatechin gallate and quercetin with spike glycoprotein (S-glycoprotein) of SARS-CoV-2: In silico study. *Biomedicines, 10*(12), Article e3074. https://doi.org/10.3390/biomedicines10123074

Alhasoon, N., Bahreini Behzadi, M. R., & Mohammadabadi, M. (2026). The effect of fennel (*Foeniculum vulgare*) on MYOD1 gene expression in the muscle tissues of the thigh, shoulder, and loin in Kermani lambs. *Journal of Livestock Science and Technologies, 14*(2), 49-56. https://doi.org/10.22103/jlst.2025.25689.1658

Arabpour, Z., Mohammadabadi, M., & Khezri, A. (2021). The expression pattern of p32 gene in femur, humeral muscle, back muscle and back fat tissues of Kermani lambs. *Agricultural Biotechnology Journal, 13*(4), 183-200. https://doi.org/10.22103/jab.2022.18782.1371

Blake, G. J., & Ridker, P. M. (2002). Inflammatory biomarkers and cardiovascular risk prediction. *Journal of Internal Medicine, 252*(4), 283-294. https://doi.org/10.1046/j.1365-2796.2002.01019.x

Bustin, S. A., Benes, V., Garson, J. A., Hellemans, J., Huggett, J., Kubista, M., Mueller, R., Nolan, T., Pfaffl, M. W., Shipley, G. L., Vandesompele, J., & Wittwer, C. T. (2009). The MIQE guidelines: Minimum information for publication of quantitative real-time PCR experiments. *Clinical Chemistry, 55*(4), 611-622. https://doi.org/10.1373/clinchem.2008.112797

Bustin, S. A. (2025). MIQE 2.0 and the urgent need to rethink qPCR standards. *International Journal of Molecular Sciences, 26*(11), Article 4975. https://doi.org/10.3390/ijms26114975

Byrne, R. A., Rossello, X., Coughlan, J. J., Barbato, E., Berry, C., Chieffo, A., Claeys, M. J., Dan, G. A., Dweck, M. R., Galbraith, M., Gilard, M., Hinterbuchner, L., Jankowska, E. A., Jüni, P., Kimura, T., Kunadian, V., Leosdottir, M., Lorusso, R., Pedretti, R. F. E., ... Ibanez, B. (2023). 2023 ESC Guidelines for the management of acute coronary syndromes. *European Heart Journal, 44*(38), 3720-3826. https://doi.org/10.1093/eurheartj/ehad191

Carmeliet, P., & Jain, R. K. (2011). Molecular mechanisms and clinical applications of angiogenesis. *Nature, 473*(7347), 298-307. https://doi.org/10.1038/nature10144

Chen, F., He, Z., Wang, C., Si, J., Chen, Z., & Guo, Y. (2024). Advances in the study of S100A9 in cardiovascular diseases. *Cell Proliferation, 57*(8), Article e13636. https://doi.org/10.1111/cpr.13636

Deveza, L., Choi, J., & Yang, F. (2012). Therapeutic angiogenesis for treating cardiovascular diseases. *Theranostics, 2*(8), 801-814. https://doi.org/10.7150/thno.4419

Duarte-Costa, S., Castro-Ferreira, R., Neves, J. S., & Leite-Moreira, A. F. (2014). S100A1: A major player in cardiovascular performance. *Physiological Research, 63*(6), 669-681. https://doi.org/10.33549/physiolres.932712

Farahvashi, M., Mohammadabadi, M., Askari-Hesni, M., Amiri Ghanatsaman, Z., & Asadollahpour Nanaei, H. (2026a). Genomic differentiation and diversity in Persian Gulf hawksbill turtles (*Eretmochelys imbricata*) revealed by the first whole-genome sequencing study. *Animals, 16*(2), Article 169. https://doi.org/10.3390/ani16020169

Farahvashi, M., Mohammadabadi, M., Askari-Hesni, M., Ghanatsaman, Z. A., & Nanaei, H. A. (2026b). Population structure of hawksbill turtles (*Eretmochelys imbricata*) nesting along the Persian Gulf coastline revealed by inter-simple sequence repeat (ISSR) markers. *Scientific Reports, 16*(1), Article 4753. https://doi.org/10.1038/s41598-025-34749-y

Faul, F., Erdfelder, E., Buchner, A., & Lang, A. G. (2009). Statistical power analyses using G*Power 3.1: Tests for correlation and regression analyses. *Behavior Research Methods, 41*(4), 1149-1160. https://doi.org/10.3758/BRM.41.4.1149

Faul, F., Erdfelder, E., Lang, A. G., & Buchner, A. (2007). G*Power 3: A flexible statistical power analysis program for the social, behavioral, and biomedical sciences. *Behavior Research Methods, 39*(2), 175-191. https://doi.org/10.3758/bf03193146

Florek, K., Mendyka, D., & Gomułka, K. (2024). Vascular endothelial growth factor (VEGF) and its role in the cardiovascular system. *Biomedicines, 12*(5), Article 1055. https://doi.org/10.3390/biomedicines12051055

Frangogiannis, N. G., Smith, C. W., & Entman, M. L. (2002). The inflammatory response in myocardial infarction. *Cardiovascular Research, 53*(1), 31-47. https://doi.org/10.1016/s0008-6363(01)00434-5

Frangogiannis, N. G. (2015). Inflammation in cardiac injury, repair and regeneration. *Current Opinion in Cardiology, 30*(3), 240-245. https://doi.org/10.1097/HCO.0000000000000158

Guan, X., Zha, L., Zhu, X., Rao, X., Huang, X., Xiong, Y., Guo, Y., Zhang, M., Zhou, D., Tu, Q., Wu, J., Wang, X., Hua, F., & Xu, J. (2025). Mechanism of action and therapeutic potential of S100A8/A9 in neuroinflammation and cognitive impairment: From molecular target to clinical application (Review). *International Journal of Molecular Medicine, 56*(4), Article 147. https://doi.org/10.3892/ijmm.2025.5588

Hajalizadeh, Z., Dayani, O., Khezri, A., Tahmasbi, R., Mohammadabadi, M., Solodka, T., Kalashnyk, O., Afanasenko, V., & Babenko, O. (2021). Expression of calpastatin gene in Kermani sheep using real-time PCR. *Journal of Livestock Science and Technology, 9*(2), 51-57. https://doi.org/10.22103/jlst.2021.18165.1381

Kazemipour, E., Sasan, H., & Mohammadabadi, M. (2025). The effect of the intrinsic resistance of *Shigella flexneri* 2a to spectinomycin on the efficiency of the CRISPR/Cas9 system. *Agricultural Biotechnology Journal, 17*(3), 177-200. https://doi.org/10.22103/jab.2025.25382.1717

Kehr, D., Ritterhoff, J., Glaser, M., Jarosch, L., Salazar, R. E., Spaich, K., Varadi, K., Birkenstock, J., Egger, M., Gao, E., Koch, W. J., Sauter, M., Freichel, M., Katus, H. A., Frey, N., Jungmann, A., Busch, C., Mather, P. J., Ruhparwar, A., ... Völkers, M. (2025). S100A1ct: A synthetic peptide derived from S100A1 protein improves cardiac performance and survival in preclinical heart failure models. *Circulation, 151*(8), 548-565. https://doi.org/10.1161/CIRCULATIONAHA.123.066961

Khabiri, A., Toroghi, R., Mohammadabadi, M., & Tabatabaeizadeh, S. E. (2025). Whole genome sequencing and phylogenetic relative of a pure virulent Newcastle disease virus isolated from an outbreak in northeast Iran. *Letters in Applied Microbiology, 78*(4), ovaf049. https://doi.org/10.1093/lambio/ovaf049

Khabiri, A., Toroghi, R., Mohammadabadi, M., & Tabatabaeizadeh, S. E. (2023). Introduction of a Newcastle disease virus challenge strain (sub-genotype VII.1.1) isolated in Iran. *Veterinary Research Forum, 14*(4), Article e221. https://doi.org/10.30466/vrf.2022.548152.3373

Khezri, A., Shafabakhsh, H., Alizadeh, A., Mohammadabadi, M., & Shakeri, M. (2025). Effects of encapsulated mixtures of plant essential oils and organic acids as an alternative to antibiotic growth promoters on humoral immune response and expression of interleukin-4 and interferon-gamma genes in broilers. *Journal of Poultry Sciences and Avian Diseases, 3*(3), 12-19. https://doi.org/10.61838/kman.jpsad.3.3.3

Kraus, C., Rohde, D., Weidenhammer, C., Qiu, G., Pleger, S. T., Völkers, M., Boerries, M., Remppis, A., Katus, H. A., & Most, P. (2009). S100A1 in cardiovascular health and disease: Closing the gap between basic science and clinical therapy. *Journal of Molecular and Cellular Cardiology, 47*(4), 445-455. https://doi.org/10.1016/j.yjmcc.2009.06.003

Ma, J., Li, Y., Li, P., Yang, X., Zhu, S., Ma, K., Gao, F., Gao, H., Zhang, H., Ma, X.-L., Du, J., & Li, Y. (2024). S100A8/A9 as a prognostic biomarker with causal effects for post-acute myocardial infarction heart failure. *Nature Communications, 15*, Article 2701. https://doi.org/10.1038/s41467-024-46973-7

Mann, D. L. (2026). In defense of homeostasis: Innate immunity in cardiac injury and repair. *Immunological Reviews, 339*(1), Article e70126. https://doi.org/10.1111/imr.70126

Martin, S. S., Aday, A. W., Almarzooq, Z. I., Anderson, C. A. M., Arora, P., Avery, C. L., Baker-Smith, C. M., Barone Gibbs, B., Beaton, A. Z., Boehme, A. K., Commodore-Mensah, Y.,

Currie, M. E., Elkind, M. S. V., Evenson, K. R., Generoso, G., Heard, D. G., Hiremath, S., Johansen, M. C., Kalani, R., ... Palaniappan, L. P. (2024). 2024 heart disease and stroke statistics: A report of US and global data from the American Heart Association. *Circulation, 149*(8), e347-e913. https://doi.org/10.1161/CIR.0000000000001209

Mohamadinejad, F., Mohammadabadi, M., Roudbari, Z., Eskandarynasab Siahkouhi, S., Babenko, O., Klopenko, N., Borshch, O., Starostenko, I., Kalashnyk, O., & Assadi Soumeh, E. (2024). Analysis of liver transcriptome data to identify the genes affecting lipid metabolism during the embryonic and hatching periods in ROSS breeder broilers. *Journal of Livestock Science and Technologies, 12*(2), 61-67. https://doi.org/10.22103/jlst.2024.23814.1554

Mohammadabadi, M., Afsharmanesh, M., Khezri, A., Kheyrodin, H., Babenko, O. I., Borshch, O., Kalashnyk, O., Nechyporenko, O., Afanasenko, V., Slynko, V., & Usenko, S. (2025). Effect of mealworm on GBP4L gene expression in the spleen tissue of Ross broiler chickens. *Agricultural Biotechnology Journal, 17*(2), 343-360. https://doi.org/10.22103/jab.2025.25277.1714

Mohammadabadi, M., Golkar, A., & Askari Hesni, M. (2023). The effect of fennel (*Foeniculum vulgare*) on insulin-like growth factor 1 gene expression in the rumen tissue of Kermani sheep. *Agricultural Biotechnology Journal, 15*(4), 239-256. https://doi.org/10.22103/jab.2023.22647.1530

Mohammadabadi, M., Kheyrodin, H., Latifi, A., & Babenko, O. I. (2022a). mRNA expression profile of DNAH1 gene in testis tissue of Raini Cashmere goat. *Agricultural Biotechnology Journal, 14*(3), 243-256. https://doi.org/10.22103/jab.2022.20199.1428

Mohammadabadi, M., Khezri, A., Afsharmanesh, M., Kheyrodin, H., Bahreini Behzadi, M. R., Babenko, O., Usenko, S., & Momen, M. (2025). Investigation of interleukin-6 gene expression in liver and spleen tissues of broiler chickens fed mealworm, probiotics, and mealworm with probiotics. *Agricultural Biotechnology Journal, 17*(4), 469-486. https://doi.org/10.22103/jab.2025.26228.1793

Mohammadabadi, M., Shaban Jorjandy, D., Arabpoor Raghabadi, Z., Abareghi, F., Sasan, H. A., & Bordbar, F. (2022b). The role of fennel on DLK1 gene expression in sheep heart tissue. *Agricultural Biotechnology Journal, 14*(2), 155-170. https://doi.org/10.22103/jab.2022.19402.1399

Noori, A. N., Behzadi, M. R. B., & Mohammadabadi, M. R. (2017). Expression pattern of Rheb gene in Jabal Barez Red goat. *The Indian Journal of Animal Sciences, 87*(11), 1375-1378. https://doi.org/10.56093/ijans.v87i11.75890

Obeagu, E. I. (2025). Inflammatory cytokines and cardiac arrhythmias: From pathogenesis to potential therapies. *Annals of Medicine and Surgery, 87*(9), 5607-5613. https://doi.org/10.1097/MS9.0000000000003499

Pakgohar, N., Mohammadabadi, M., Askari Hesni, M., & Farahvashi, M. (2026). Evaluation of genetic markers for assessing sex-related differences in the hawksbill turtle (*Eretmochelys imbricata*). *Agricultural Biotechnology Journal, 18*(1), 481-498.

Petersen, J. W., & Pepine, C. J. (2015). Microvascular coronary dysfunction and ischemic heart disease: Where are we in 2014? *Trends in Cardiovascular Medicine, 25*(2), 98-103. https://doi.org/10.1016/j.tcm.2014.09.013

Pleger, S. T., Remppis, A., Heidt, B., Völkers, M., Chuprun, J. K., Kuhn, M., Zhou, R. H., Gao, E., Szabo, G., Weichenhan, D., Müller, O. J., Eckhart, A. D., Katus, H. A., Koch, W. J., & Most, P. (2005). S100A1 gene therapy preserves in vivo cardiac function after myocardial

infarction. *Molecular Therapy, 12*(6), 1120-1129. https://doi.org/10.1016/j.ymthe.2005.08.002

Postollec, F., Falentin, H., Pavan, S., Combrisson, J., & Sohier, D. (2011). Recent advances in quantitative PCR (qPCR) applications in food microbiology. *Food Microbiology, 28*(5), 848-861. https://doi.org/10.1016/j.fm.2011.02.008

Ritterhoff, J., & Most, P. (2012). Targeting S100A1 in heart failure. *Gene Therapy, 19*(6), 613-621. https://doi.org/10.1038/gt.2012.8

Rohde, D., Ritterhoff, J., Voelkers, M., Katus, H. A., Parker, T. G., & Most, P. (2010). S100A1: A multifaceted therapeutic target in cardiovascular disease. *Journal of Cardiovascular Translational Research, 3*(5), 525-537. https://doi.org/10.1007/s12265-010-9211-9

Roudbar, M. A., Mohammadabadi, M., & Salmani, V. (2015). Epigenetics: A new challenge in animal breeding. *Genetics in the Third Millennium, 12*(4), 3900-3914.

Safaei, S. M. H., Dadpasand, M., Mohammadabadi, M., Atashi, H., Stavetska, R., Klopenko, N., & Kalashnyk, O. (2022). An *Origanum majorana* leaf diet influences myogenin gene expression, performance, and carcass characteristics in lambs. *Animals, 13*(1), Article 14. https://doi.org/10.3390/ani13010014

Safaei, S. M. H., Mohammadabadi, M., Moradi, B., Kalashnyk, O., Klopenko, N., Babenko, O., Borshch, O. O., & Afanasenko, V. (2024). Role of fennel (*Foeniculum vulgare*) seed powder in increasing testosterone and IGF1 gene expression in the testis of lamb. *Gene Expression, 23*(2), 98-105. https://doi.org/10.14218/GE.2023.00020

Sun, Y., Xu, H., Gao, W., Deng, J., Song, X., Li, J., & Liu, X. (2024). S100a8/A9 proteins: Critical regulators of inflammation in cardiovascular diseases. *Frontiers in Cardiovascular Medicine, 11*, Article 1394137. https://doi.org/10.3389/fcvm.2024.1394137

Taylor, S. C., & Mrkusich, E. M. (2014). The state of RT-quantitative PCR: Firsthand observations of implementation of minimum information for the publication of quantitative real-time PCR experiments (MIQE). *Journal of Molecular Microbiology and Biotechnology, 24*(1), 46-52. https://doi.org/10.1159/000356189

Taylor, S. C., Nadeau, K., Abbasi, M., Lachance, C., Nguyen, M., & Fenrich, J. (2019). The ultimate qPCR experiment: Producing publication quality, reproducible data the first time. *Trends in Biotechnology, 37*(7), 761-774. https://doi.org/10.1016/j.tibtech.2018.12.002

Vogl, T., Eisenblätter, M., Völler, T., Zenker, S., Hermann, S., van Lent, P., Faust, A., Geyer, C., Petersen, B., Roebrock, K., Schäfers, M., Bremer, C., & Roth, J. (2014). Alarmin S100A8/S100A9 as a biomarker for molecular imaging of local inflammatory activity. *Nature Communications, 5*, Article 4593. https://doi.org/10.1038/ncomms5593

Zhou, Y., Zha, Y., Yang, Y., Ma, T., Li, H., & Liang, J. (2023). S100 proteins in cardiovascular diseases. *Molecular Medicine, 29*(1), Article 68. https://doi.org/10.1186/s10020-023-00662-1

Zygiel, E. M., & Nolan, E. M. (2019). Exploring iron withholding by the innate immune protein human calprotectin. *Accounts of Chemical Research, 52*(8), 2301-2308. https://doi.org/10.1021/acs.accounts.9b00250

مجله بیوتکنولوژی کشاورزی
شاپا چاپی: ۶۷۰۵-۲۲۲۸ شاپا الکترونیکی: ۶۵۰۰-۲۲۲۸
دانشگاه شهید باهنر کرمان
انجمن بیوتکنولوژی ایران

تحلیل یکپارچه بیان پروتئینی و ژنی S100A1 و S100A8/A9 نشان‌دهنده اختلال هماهنگ در هموستاز کلسیم، فعال‌سازی ایمنی ذاتی و سیگنالینگ آنژیوژنیک در انفارکتوس حاد میوکارد

الهام فاضل حمزه

* نویسنده مسئول. گروه بیوشیمی بالینی، دانشکده پزشکی حمورابی، دانشگاه بابل، حله، عراق. ایمیل: if0261758@gmail.com

عبدالسمیع حسن الطائی

دانشکده پزشکی، دانشگاه بابل، حله، عراق. ایمیل: abdulsamie68@gmail.com

امیر الجبوی

دانشکده پزشکی، دانشگاه بابل، حله، عراق. ایمیل: aljubawiiameer1981@gmail.com

تاریخ دریافت: ۱۴۰۵/۰۱/۰۱ تاریخ دریافت فایل اصلاح شده نهایی: ۱۴۰۵/۰۲/۲۷ تاریخ پذیرش: ۱۴۰۵/۰۲/۲۸

چکیده

هدف: انفارکتوس حاد میوکارد (AMI) با تعاملات مولکولی پیچیده‌ای مشخص می‌شود که شامل اختلال در هموستاز کلسیم در کاردیومیوسیت‌ها، فعال‌سازی مسیرهای ایمنی ذاتی و اختلال در سیگنالینگ آنژیوژنیک است. با این حال، ارتباط یکپارچه بین پروتئین اختصاصی کاردیومیوسیت S100A1 و کمپلکس التهابی S100A8/A9 هنوز به‌طور کامل شناخته نشده است. بنابراین، هدف این مطالعه بررسی الگوهای بیان پروتئینی و ژنی S100A1 و S100A8/A9 و ارتباط آن‌ها با نشانگرهای التهابی (TNF-α) و آنژیوژنیک (VEGF-A) در AMI بود.

مواد و روش‌ها: این مطالعه مورد–شاهدی شامل ۱۷۶ شرکت‌کننده (۸۸ بیمار مبتلا به AMI و ۸۸ فرد سالم همسان از نظر سن و جنس) بود. شرکت‌کنندگان از بیمارستان آموزشی الحله و شهر پزشکی مرجان انتخاب شدند. سطوح سرمی S100A1، S100A8/A9، TNF-α و VEGF-A با روش ELISA اندازه‌گیری شد، در حالی که کلسیم سرم با روش اسپکتروفتومتری تعیین گردید. میزان بیان ژنی S100A1، S100A8 و S100A9 با استفاده از qRT-PCR و روش $2^{-\Delta\Delta Ct}$ بررسی شد. همچنین برای ارزیابی عملکرد تشخیصی از تحلیل منحنی ROC استفاده گردید.

نتایج: اختلال چندمحوری قابل توجهی در بیماران AMI مشاهده شد. بیان mRNA ژن S100A1 به‌طور معنی‌داری کاهش یافت ($p<0.0001$) و همزمان سطح پروتئین آن نیز کاهش نشان داد (AUC = 0.69Y, specificity = 100%). در مقابل، نشانگرهای التهابی افزایش یافتند و کمپلکس S100A8/A9 عملکرد تشخیصی قابل قبولی نشان داد (AUC=0.76)، در حالی که TNF-α قدرت تفکیک تشخیصی نداشت (AUC=0.50). کلسیم سرم دقت تشخیصی بالایی نشان داد (AUC=0.82) که بیانگر اختلال زودهنگام در هموستاز کلسیم بود. اختلال آنژیوژنیک با کاهش VEGF-A مشخص شد، اما ارزش تشخیصی محدودی داشت (AUC = 0.54). تحلیل بیان ژنی همچنین افزایش معنی‌دار S100A8 ($p=0.030$) و S100A9 ($p=0.044$) را تأیید کرد. هیچ همبستگی معنی‌داری بین S100A1 و نشانگرهای التهابی مشاهده نشد ($p>0.05$)، در حالی که بین S100A8 و S100A9 همبستگی مثبت قوی وجود داشت که نشان‌دهنده فعال‌سازی هماهنگ التهابی است.

نتیجه‌گیری: یافته‌ها نشان می‌دهند که تنظیم کلسیم مرتبط با S100A1، پاسخ‌های ایمنی ناشی از S100A8/A9 و اختلال در آنژیوژنز مرتبط با VEGF-A به‌طور همزمان در انفارکتوس حاد میوکارد درگیر هستند. قدرت تشخیصی بالاتر S100A1 نشان می‌دهد که نشانگرهای مرتبط با تنظیم کلسیم در سلول‌های قلبی می‌توانند در تشخیص بهتر AMI نسبت به شاخص‌های التهابی سنتی نقش مهم‌تری داشته باشند.

کلمات کلیدی: انفارکتوس حاد میوکارد، کلسیم، بیان ژن، TNF-α، VEGF-A

نوع مقاله: پژوهشی

استناد: الهام فاضل حمزه، عبدالسمیع حسن الطائی، امیر الجبوی (۱۴۰۵) تحلیل یکپارچه بیان پروتئینی و ژنی S100A1 و S100A8/A9نشان‌دهنده اختلال هماهنگ در هموستاز کلسیم، فعال‌سازی ایمنی ذاتی و سیگنالینگ آنژیوژنیک در انفارکتوس حاد میوکارد. *مجله بیوتکنولوژی کشاورزی*، ۱۸(۳)، ۴۷۷-۵۰۴.

Publisher: Shahid Bahonar University of Kerman & Iranian Biotechnology Society.